

Synthesis and Characterization of a Series of Smectic Liquid Crystalline Elastomers

Xiao-Zhi He, Bao-Yan Zhang, Ling-Jiu Xiao, Yang Wang, Hai-Quan Wu

Center for Molecular Science and Engineering, Northeastern University, Shenyang 110004, People's Republic of China

Received 21 October 2004; accepted 10 December 2004

DOI 10.1002/app.21767

Published online in Wiley InterScience (www.interscience.wiley.com).

ABSTRACT: A series of new smectic and cholesteric liquid crystalline elastomers was prepared by graft polymerization of mesogenic monomer with the chiral and nonmesogenic crosslinking agent using polymethylhydrosiloxane as backbone. The chemical structures of the monomers and polymers obtained were confirmed by Fourier transform infrared (FTIR), proton nuclear magnetic resonance spectra ($^1\text{H-NMR}$). The mesomorphic properties were investigated by differential scanning calorimetry (DSC), polarizing optical microscopy (POM), and X-ray diffraction measurements (XRD). M_1 showed smectic (S_B , S_C , S_A) and nematic phases during the heating and the cooling cycles. Polymer P_0 and elastomer P_1 exhibited smectic B phase, elastomers P_2 – P_5 showed smectic A phase, P_6 and P_7 showed cholesteric

phase, and P_8 displayed stress-induced birefringence. The elastomers containing less than 15 mol % M_2 displayed elasticity and reversible phase transition with wide mesophase temperature ranges. Experimental results demonstrated that the glass transition temperatures decreased first and then increased; melting temperatures and the isotropization temperatures and the mesophase temperature ranges decreased with increasing content of crosslinking unit. © 2005 Wiley Periodicals, Inc. *J Appl Polym Sci* 97: 498–506, 2005

Key words: smectic liquid crystalline; chiral; crosslinking; elastomers; synthesis

INTRODUCTION

It is well known that liquid crystalline elastomers (LCEs), combining the properties LC phase with rubber elasticity, have received much attention since the synthesis of LCEs was reported in 1981.^{1–7} Recently, smectic C(SmC) elastomers composed of chiral materials have attracted both industrial and scientific interests because of their additional properties, such as piezoelectricity, ferroelectricity, and pyroelectricity. Chiral smectic C(S_C^*) elastomers can be obtained by the combination of a chiral component and a mesogenic crosslinking unit.^{8–11} Consequently, cholesteric liquid crystalline elastomers (cholesteric LCEs) have been considered as candidates for the fabrication of piezoelectric devices.^{12–18} Our group has done much research in the field of cholesteric LCEs.^{19–21} In our previous research, cholesteric LCEs were obtained by introducing chiral crosslinking agents and nematic LC monomers, so we investigated whether S_C^* elastomers can be obtained by introducing chiral crosslinking agents and smectic monomers. In general, side-chain S_C^* elastomers were usually obtained by containing chiral mesogenic or nonmesogenic units with non-chiral crosslinking agents. The present article deals

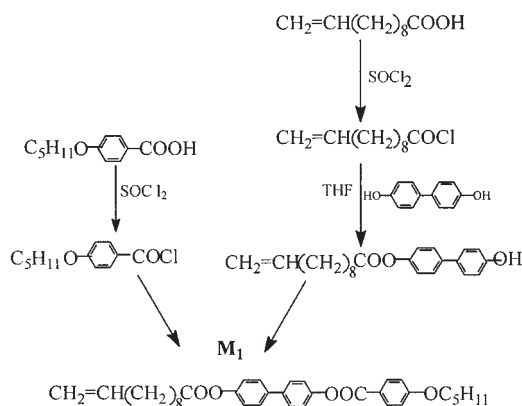
with a new preparation of a side-chain LCEs with pendant smectic–nematic monomer groups (M_1 , pentyloxy-4-undecanoyloxy-4'-benzoate) and chiral and nonmesogenic crosslinking agents (M_2 , isosorbide 4-allyloxybenzoyl bisate), which link directly to the polymethylhydrosiloxane backbone with flexible spacers. We expected to obtain S_C^* or cholesteric LCEs by the method. The reason we chose isosorbide is that it possesses a high twisting power and can better introduce chirality into LCEs.²² However, to the best of our knowledge, few S_C^* or cholesteric LCE materials bearing chiral crosslinking agents have been described so far; it is necessary and significant to synthesize and discuss various kinds of side-chain cholesteric or S_C^* LCEs with chiral crosslinking agents to explore their potential application.

EXPERIMENTAL

Materials

Polymethylhydrosiloxane (PMHS, $M_n = 700$ – 800) was purchased from Jilin Chemical Industry Co. (China). 4,4'-Biphenol was purchased from Beijing Chemical Industry Co. (China). Undecylenic acid was purchased from Beijing Jinlong Chemical Reagent Co. Ltd (China). Isosorbide was bought from Yangzhou Shenzhou New Material Co. Ltd (China). 1-Bromopentane was obtained from Yancheng Longsheng Fine Chemical Industry Co.(China). Ethyl 4-hydroxyl

Correspondence to: B.Y. Zhang (baoyanzhang@hotmail.com).



Scheme 1 Synthetic route of monomers.

benzoate was purchased from Shenyang Xinxu Chemical Reagent Company (China). Toluene used in the hydrosilycation reaction was first refluxed over sodium and then distilled under nitrogen. All other solvents and reagents were purified by standard methods.

Characterization

IR spectra were measured on a Perkin-Elmer spectrum one FT-IR spectrometer (Perkin-Elmer Instruments, USA). $^1\text{H-NMR}$ spectra (300 MHz) were recorded on a Varian WH-90PFT spectrometer (Palo Alto, CA). Specific rotation was performed with a Perkin-Elmer 341 polarimeter (Perkin-Elmer Instruments, England). Phase transition temperatures and thermodynamic parameters were determined by using a Netzsch DSC 204 (Netzsch, Germany) with a liquid nitrogen cooling system. The heating and cool-

ing rates were $10^\circ\text{C}/\text{min}$. A Leica DMRX (Leica, Germany) polarizing optical microscope equipped with a Linkam THMSE-600 (Linkam, England) hot stage was used to observe phase transition temperatures and to analyze LC properties for the monomers and polymers through observation of optical textures. XRD measurements were performed with a nickel-filtered $\text{Cu-K}\alpha$ ($\lambda = 0.1542 \text{ nm}$) radiation with a DMAX-3A Rigaku (Rigaku, Japan) powder diffractometer.

Synthesis of the monomers

The synthesis of the olefinic monomers is shown in Scheme 1.

4-undecanoyloxy-4'-hydroxy biphenyl

37.2 g (0.2mol) of 4,4'-hydroxybiphenyl was dissolved in pyridine (150 mL) and then 10.7 g (0.05mol) of undecylenic acid chloride (laboratory synthesized) was added dropwise to the cold mixture. After stirring for 12 h at 50°C , the cold reaction mixture was precipitated into water and acidified to pH 1 with hydrochloric acid. The produced precipitate was filtered and washed with water to neutrality. After stirring in warm dilute alkali liquor, the crude product was washed with water and recrystallized three times from ethanol. White solid powders were obtained (yield 20%; mp 122°C).

IR(KBr): 3490 ($-\text{OH}$), 2980–2850 ($-\text{CH}_3, -\text{CH}_2$), 1727 ($\text{C}=\text{O}$), 1648 ($\text{C}=\text{C}$), 1605–1450 (Ar-)

Pentyloxy-undecanoyloxy-4'-benzoate (M_1)

A few drops of *N,N*-dimethylformamide (DMF) were added to a suspension of 4-pentyloxy-benzoic acid (0.1

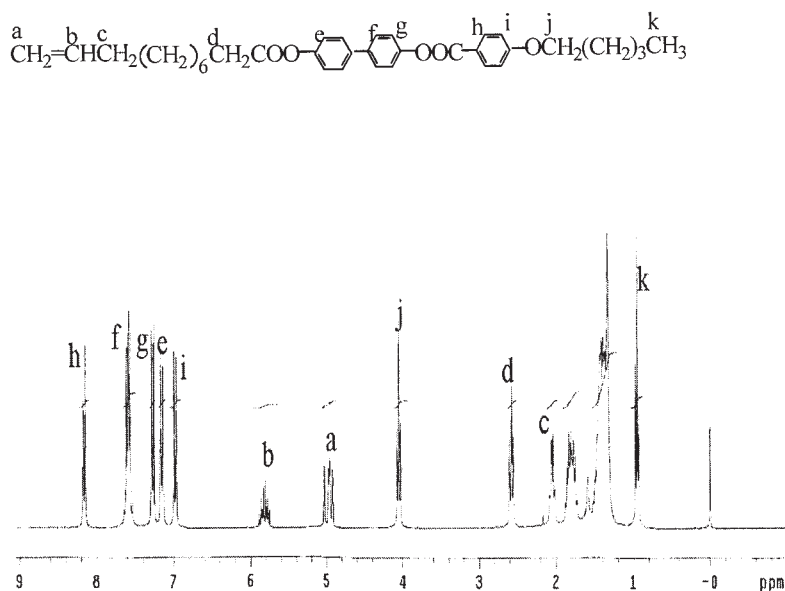
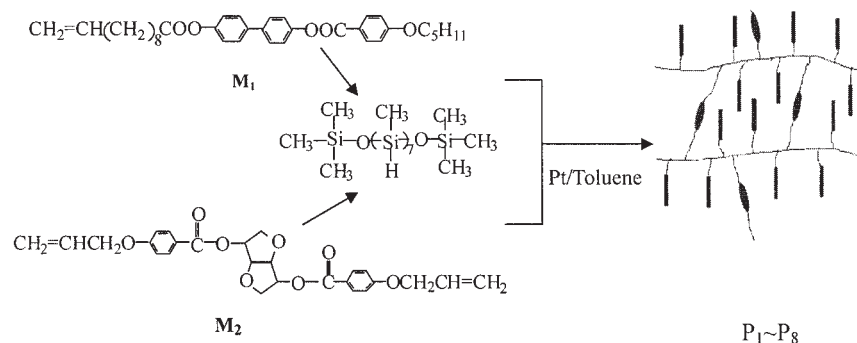


Figure 1 $^1\text{H-NMR}$ spectra of M_1 .



Scheme 2 Synthesis and schematic representation of elastomers.

mol) (laboratory synthesized) in freshly distilled thionyl chloride (40 mL) and the reaction mixture was refluxed for 5 h and then the excess thionyl chloride was removed under reduced pressure to give the corresponding acid chloride. 4-Undecanoyloxy-4'-hydroxy biphenyl (0.1 mol) was dissolved in a mixture of dry pyridine (10 mL) and dry tetrahydrofuran (100 mL); the 4-pentyloxy-benzoic acid chloride was then added at once and the reaction mixture was refluxed for 24 h. The cold reaction mixture was precipitated into water and the precipitated product was isolated by filtration and was recrystallized from ethanol (yield 72%; mp 100.2°C). In Figure 1 the $^1\text{H-NMR}$ spectra of M_1 are shown.

IR (KBr): 3078, 3038 (=C-H), 2980–2850 ($-\text{CH}_3$, $-\text{CH}_2$), 1745, 1727 (COO), 1648 (C=C), 1605–1450 (Ar-), 1258 cm^{-1} (C–O–C).

$^1\text{H-NMR}$ (CDCl_3 , δ): 0.93–0.97 (t, 3H, $-\text{CH}_3$), 1.33–1.86 (m, 18H, $-(\text{CH}_2)_6$, $-(\text{CH}_2)_3$), 2.02–2.08 (m, 2H, $\text{CH}_2=\text{CHCH}_2$), 2.55–2.60 (t, 2H, $-\text{CH}_2\text{COO}$) 4.03–4.07 (t, 2H, $-\text{OCH}_2$), 4.92–5.03 (m, 2H, $\text{CH}_2=\text{CH}$), 5.75–5.88 (m, 1H, $\text{CH}_2=\text{CH}$), 6.96–8.17 (m, 12H, Ar-H).

Synthesis of isosorbide 4-allyloxybenzoyl bisate (M_2)

M_2 was prepared according to the literature procedures reported by He et al.²³ (yield 34%; mp 96°C; $[\alpha]_{589}^{17.2} = -75.5^\circ$

IR(KBr): 3038 (=C-H), 2980, 2850 ($-\text{CH}_3$, $-\text{CH}_2$), 1716 (C=O), 1638 (C=C), 1605–1450 cm^{-1} (Ar-).

$^1\text{H-NMR}$ (CDCl_3 , δ): 4.00–5.04 (m, 10H, isosorbide), 4.59–4.68 (d, 2H, $\text{CH}_2=\text{CHCH}_2\text{O}$), 5.31–5.46 (m, 2H, $\text{CH}_2=\text{CH}$) 6.92–8.06 (m, 8H, Ar-H)

Synthesis of the polymers

The synthetic ways of uncrosslinked and crosslinked polymers (elastomers) are similar. The synthetic route of elastomers is outlined in Scheme 2. The mesogenic monomer and the different content of the chiral crosslinking agent reacted with Si-H of PMHS to form elastomers in the presence of Pt catalyst.²⁰ All polymers synthesized are listed in Table I. The products were dried in a vacuum at room temperature.

IR(KBr): 2980, 2850 ($-\text{CH}_3$, $-\text{CH}_2$), 1732 (C=O), 1605–1450 (Ar-), 1200–1000 cm^{-1} (Si–O–Si)

RESULTS AND DISCUSSION

Synthesis

The novel monomer, a smectic and nematic liquid crystalline (M_1), and a chiral crosslinking agent (M_2), have been synthesized. The reaction pathways to the

TABLE I
Polymerization of P_0 – P_8

Polymer	Feed (mmol)		M_2^a (mol %)	Yield (%)	Solubility ^b		
	M_1	M_2			Toluene	Xylene	DMF
P_0	3.500	0.000	0	86.5	+	+	+
P_1	3.360	0.070	2	82.3	–	–	–
P_2	3.220	0.140	4	84.7	–	–	–
P_3	3.080	0.210	6	79.0	–	–	–
P_4	2.940	0.280	8	80.2	–	–	–
P_5	2.800	0.350	10	75.3	–	–	–
P_6	2.660	0.420	12	71.3	–	–	–
P_7	2.450	0.525	15	65.3	–	–	–
P_8	2.100	0.700	20	60.2	–	–	–

^a Molar fraction of M_2 based on $M_1 + M_2$.

^b +, dissolve; –, insolubility or swelling.

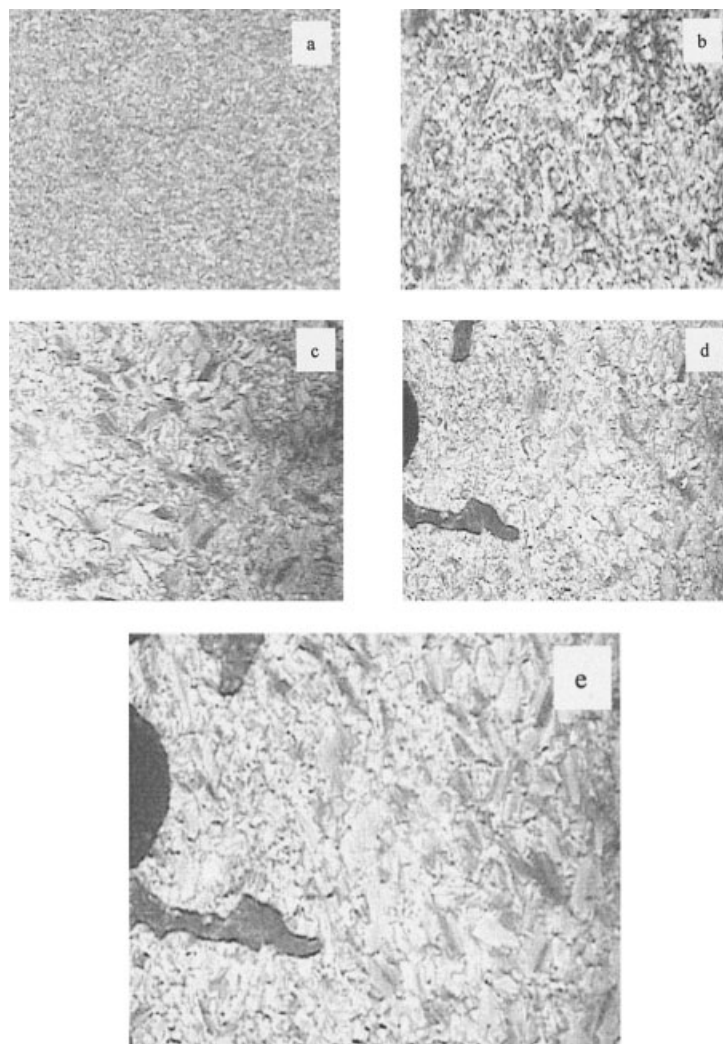


Figure 2 Optical texture of monomer M_1 ($\times 200$). (a) Grainy texture of M_1 at heating to 139.6°C ; (b) threaded-like texture of M_1 at heating to 197.7°C ; (c) focal-conic of M_1 at cooling to 132.6°C ; (d) broken focal-conic texture of M_1 at cooling to 104.2°C ; (e) focal-conic texture of M_1 at cooling to 97.6°C .

M_1 and M_2 are shown in Scheme 1. M_1 was prepared by (1) monoesterification of 4,4'-hydroxy-biphenyl with undecylenic acid chloride to give 4-undecanoyloxy-4'-hydroxy biphenyl and (2) esterification of 4-pentyloxy-benzoic acid chloride with 4-undecanoyloxy-4'-hydroxy biphenyl to give M_1 . M_2 was prepared by (1) etherification of 4-hydroxy-benzoic acid with 3-bromopropene to give 4-allyloxy benzoic acid and (2) esterification of 4-allyloxy benzoic acid chloride with isosorbide to give M_2 . The chemical structures of the two monomers were characterized by FTIR and $^1\text{H-NMR}$ spectroscopy. The FTIR of M_1 and M_2 , respectively, showed characteristic bands at $1742\text{--}1727\text{ cm}^{-1}$ originating from ester $\text{C}=\text{O}$ stretching, and $1648\text{--}1640\text{ cm}^{-1}$ due to olefinic $\text{C}=\text{C}$ stretching, and $1605\text{--}1450\text{ cm}^{-1}$ corresponding to aromatic $\text{C}=\text{C}$ stretching. The $^1\text{H-NMR}$ spectra of M_1 and M_2 showed multiplets at 6.92–8.17, 5.31–6.20, 4.92–5.46, 4.00–4.68, and 0.97–2.6 ppm corre-

sponding to aromatic, vinyl, methyleneoxy, and methyl, methylene protons. The new series of elastomers $P_1\text{--}P_8$ was prepared by a one-step hydrozylation reaction between Si-H groups of PMHS and olefinic $\text{C}=\text{C}$ of smectic and nematic monomers and the difunctional chiral crosslinking agent in toluene, using hexachloroplatinate as catalyst at 60°C . The yields and properties of $P_0\text{--}P_8$ are summarized in Table I. The obtained elastomers $P_1\text{--}P_7$ were insoluble in toluene, xylene, DMF, chloroform etc., but could swell in these solvents. The FTIR spectra of $P_0\text{--}P_8$ showed the complete disappearance of the Si-H stretching band at 2166 cm^{-1} . Characteristic absorption bands appeared at 1732, 1605–1450, and $1200\text{--}1000\text{ cm}^{-1}$ attaching to the stretching of ester $\text{C}=\text{O}$, aromatic, and Si-O-Si, respectively. It can be concluded that the chemical structures of the obtained monomers and polymers are consistent with our expectation.

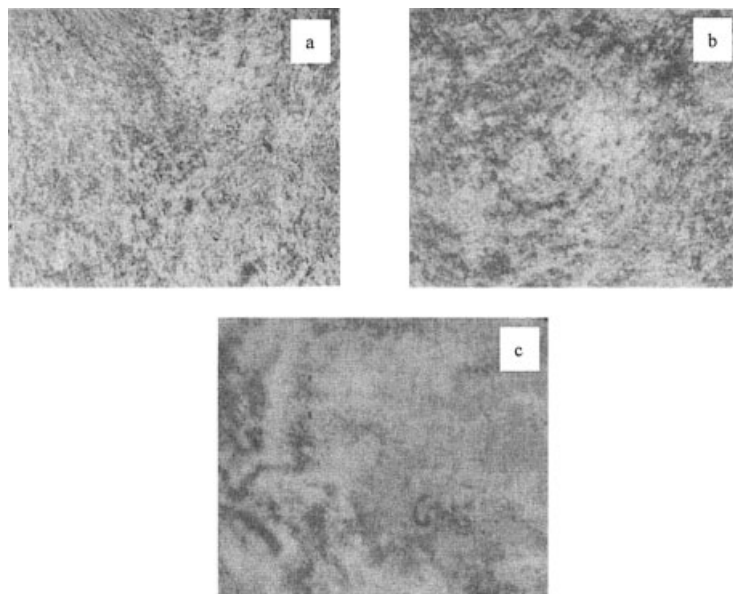


Figure 3 Optical texture of polymers ($\times 200$). (a) Texture of P_0 at heating to 195.3°C ; (b) step partial texture of P_4 at heating to 191.4°C ; (c) Grandjean texture of P_6 at heating to 163°C .

Optical analysis

The optical textures of the monomers and polymers were characterized by POM with hot stage under nitrogen atmosphere. The visual observation under POM has revealed that M_1 exhibited an enantiotropic smectic–nematic phase. When M_1 was heated to 100.0°C , the sample began to melt and flow and gradually appeared with a grainy texture, which is the texture of the smectic phase. With continued heating to 146.0°C , the typical nematic threaded texture gradually appeared and remained until 200.0°C . On the cooling process, the texture of M_1 underwent threaded texture at 197.8°C , focal–conic texture (S_A) at 146.1°C , broken focal–conic texture (S_C) at 110.0°C , and focal–conic texture (S_B) again at 102.0°C . Photomicrographs are shown in Figure 2(a–e), respectively. On the first heating, we could not observe obvious changes on different smectic textures, but, on the second heating, we observed the different texture changes of smectic texture just like the first cooling. This should be due to the regular molecular arrangement on the second heating. The results suggested that M_1 showed smectic (S_B , S_C , S_A) phase and nematic phase on the heating cycle and the subsequent cooling cycle. Photomicrographs of polymers are shown in Figure 3(a–c), respectively. The uncrosslinked polymer P_0 and crosslinked polymer P_1 showed bright color, but the textures of them cannot be clearly made out. Elastomers P_2 – P_5 exhibited smectic step particle textures, while P_6 , and P_7 showed Grandjean texture and P_8 displayed stress-induced birefringence. The

type of LC phase of polymers should be further characterized by X-ray diffraction

Thermal analysis

Analysis of monomer M_1

The DSC curve and phase transition temperature of M_1 during heating and cooling runs are shown in Figure 4 and Table II. As we all know, when there is a small molecular weight liquid crystalline occurred phase transition, there will be strict enthalpy changes, which are the direct report of the degree of acting force between liquid crystalline molecule and ordered arrangement. The heating cycle thermogram showed four clear endotherms at 100.2 , 111.3 , 148.3 , 200.1°C and one small endotherms at 104.3°C . In the subsequent cooling cycle, there were five corresponding endotherms at 197.8 , 146.1 , 109.2 , 102.1 , and 66.8°C . The DSC measurements reveal a melting to smectic B (S_B) at 100.2°C , a transition from S_B to smectic C (S_C) at 104.3°C , a change from S_C to smectic A (S_A) at 111.3°C , a transformation from S_A to nematic at 148.3°C , and a clearing at 200.1°C . On cooling from the isotropic phase into nematic at 197.8°C , nematic to S_A at 146.1°C , S_A to S_C at 109.2°C , S_C to S_B at 102.1°C and S_B to crystal at 66.8°C . As seen from Figure 4, the values of the enthalpy changes from nematic to smectic phase and between the smectic phase are small. Monomer M_1 is enantiotropy liquid crystalline. The results of optical and thermal analysis are consistent.

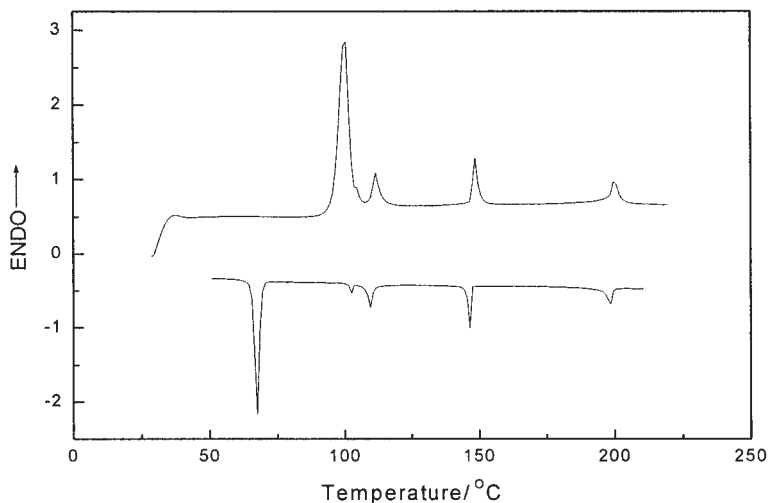


Figure 4 DSC thermographs of liquid crystal monomer M_1 .

Analysis of polymer and elastomers

Liquid crystalline polymers (LCP) can be divided into amorphous LCP, semicrystallized LCP, and crystallized LCP. The mesomorphic temperature range of semicrystallized and crystallized LCP is between the melting and the clearing temperature. The principles are fit for LCEs. Representative DSC curves of elastomers, obtained on the second heating scan, are presented in Figure 5. Phase transition temperatures and the results of thermal analysis are shown in Table III, and the effect of the content of crosslinking units on the phase transition are shown in Figure 6.

On the second heating scan of elastomers (Figure 5), it shows a glass transition temperature, a melting point, and the temperature of mesophase to isotropic phase transition. All transitions are reversible and do not change on repeated heating and cooling cycles. The phase transition temperatures noted in DSC thermograms are consistent with the mesomorphic transition temperatures observed by POM, revealing that elastomers are semicrystallized.

As seen from the data in Table III and Figure 6, T_g values decreased first and then increased with the increase of the content of chiral crosslinking agent.

The influent factors to T_g are summarized as the property of polymer backbone, the rigidity of mesogenic unit, the flexible spacer length, and the content of crosslinking agent. The polysiloxane backbone and mesogenic unit with a long, flexible spacer inclines to reduce T_g value, while the crosslinking agent has two opposite actions: crosslinking and plasticization. Crosslinking imposes additional constraints on the segment motion of polymer chains and might be expected to raise the glass transition temperature. Plasticization inclines to reduce the glass transition temperature. When the content of crosslinking agent is less than certain critical, the plasticization effect is predominant; otherwise the crosslinking effect is a main factor. It can be seen from Table III that the T_g value of P_0 - P_4 was reduced from 68.0 to 54.6°C, which is the influence of plasticization; the T_g value of P_5 - P_8 increased from 55.7 to 61.2°C, from which it can be concluded that the crosslinking effect gradually became predominant when the content of crosslinking agent reached critical value.

On the DSC curves of P_0 - P_7 , another peak of heat absorption can be found, which is melting temperature (T_m). On one hand, the flexibility of the mesomor-

TABLE II
Phase Transition of Monomer M_1

	Phase transition ^{a,b} (°C)
Heating	K100.2(25.4) S _B 104.3S _C 111.3(3.6)S _A 148.3(4.0) N200.1(2.0) I
Cooling	I197.8(2.3) N146.1(4.2) S _A 109.2(3.0) S _C 102.1(0.7)S _B 66.8(23.0) K

^a K, solid; N, nematic; S_A, smectic A; S_B, smectic B; S_C, smectic C; I, isotropic.

^b Corresponding enthalpy changes in $J \cdot g^{-1}$ are in parentheses.

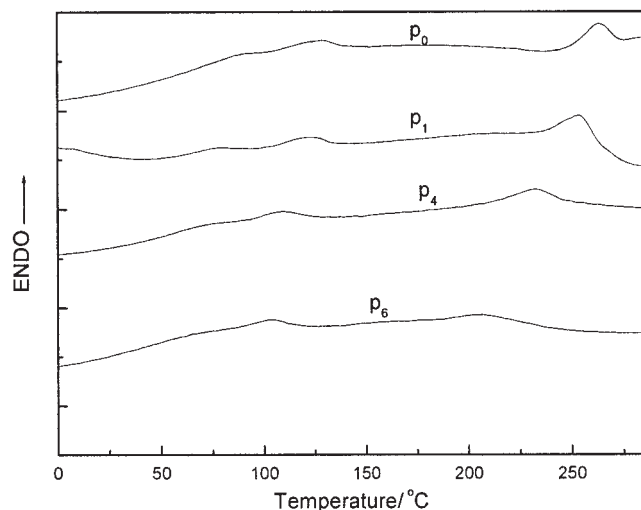


Figure 5 DSC thermographs of liquid crystal elastomers.

phic monomer and the crosslinking agent can easily arrange the elastomer into order when it possesses crystallization tendency²⁴ and the T_m value will increase; on the other hand, crosslinking action will confine the motion of molecule chain and result in the decrease of crystalline ability and the T_m value will be reduced. The two factors interacted and the T_m value of P_0 – P_7 was reduced from 128.6 to 102.3°C.

Similar to T_g , crosslinking may influence the clearing point (T_i) in two ways. First, crosslinking units may act as a nonmesogenic diluent and lead to a downward shift in the clearing point as increasing contents are added to a LC polymer. For a crosslinked sample, chemical crosslinking could prevent the motion and orientation of the mesogenic molecule and was not in favor of the mesogenic orientation in the elastomers with increasing the content of crosslinking agent. Second, for a crosslinked sample, heating to the isotropic state required additional energy to distort the polymer backbone from the anisotropic state at crosslinking and led to forward shift in the clearing point with

TABLE III
Thermal Properties of Polymers P_0 – P_8

Polymer	T_g (°C)	T_m (°C)	T_i (°C)	ΔH (J · g ⁻¹)	ΔT^a (°C)
P_0	68.0	128.6	263.6	3.39	135.0
P_1	64.1	121.0	253.4	3.37	132.4
P_2	61.8	120.0	250.4	2.62	130.4
P_3	61.7	114.1	240.5	2.86	126.4
P_4	54.6	110.6	237.3	2.29	126.7
P_5	55.7	110.0	228.4	2.17	118.4
P_6	56.8	102.6	207.8	1.58	105.2
P_7	57.3	102.3	186.6	1.26	84.3
P_8	61.2	—	—	—	—

^a Mesophase temperature ranges (T_i – T_m).

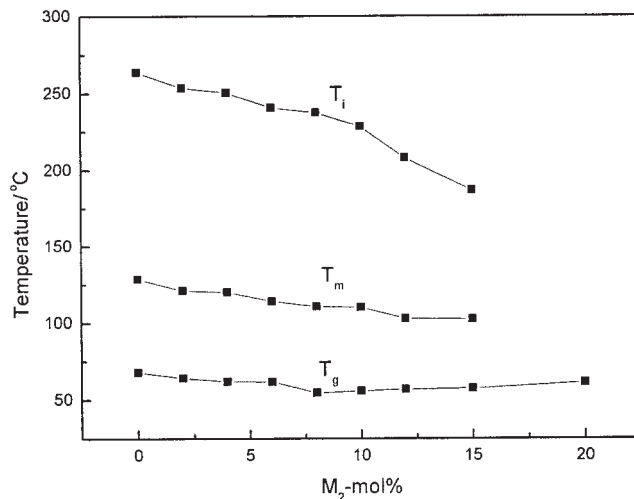


Figure 6 Effect of M_2 content on phase transition temperature of the elastomers.

increasing contents of chiral crosslinking agent. In this study, the non-LC crosslinking agent is induced into polymer backbone, so the first factor is predominant. It can be seen that the T_i value is reduced with the increasing content of crosslinking agent. When the concentration of crosslinking units increased from 0 to 15%, the T_i value of P_0 – P_7 decreased from 263.6 to 186.6°C, and, at the same time, P_0 – P_7 displayed wide mesophase temperature ranges (ΔT) from 135.0 to 84.3°C. ΔT values of elastomers decreased with increasing the contents of the crosslinking agent. The DSC curve of P_8 only showed a glass transition and no melting temperature or mesophase to isotropic transition due to high levels of crosslinking, which reduced the ability of crystallization and disturbed the LC order. The reported thermal and phasic results are also consistent with results for similar classes of polymers.²⁵

X-ray diffraction

XRD analysis allowed for a complementary assessment of the nature of the phases observed by DSC and POM, giving additional information about their structural parameters. WAXD patterns of elastomers are shown in Figure 7. The X-ray diffraction pattern of the quenched polymer P_0 – P_5 films first showed a sharp reflection peak at 2θ of 5.11–4.22° ($d = 19.20$ – 22.78 Å) and other reflection peaks that are sharp at first and then broad at 2θ of 7.52–6.76° ($d = 13.30$ – 14.51 Å). The first peak corresponds to the smectic layer spacing, which was close to molecular lengths of the fully stretched mesomorphic units that were calculated to be 20.45 Å. The other peak around 7.0° in each diffraction pattern seems to

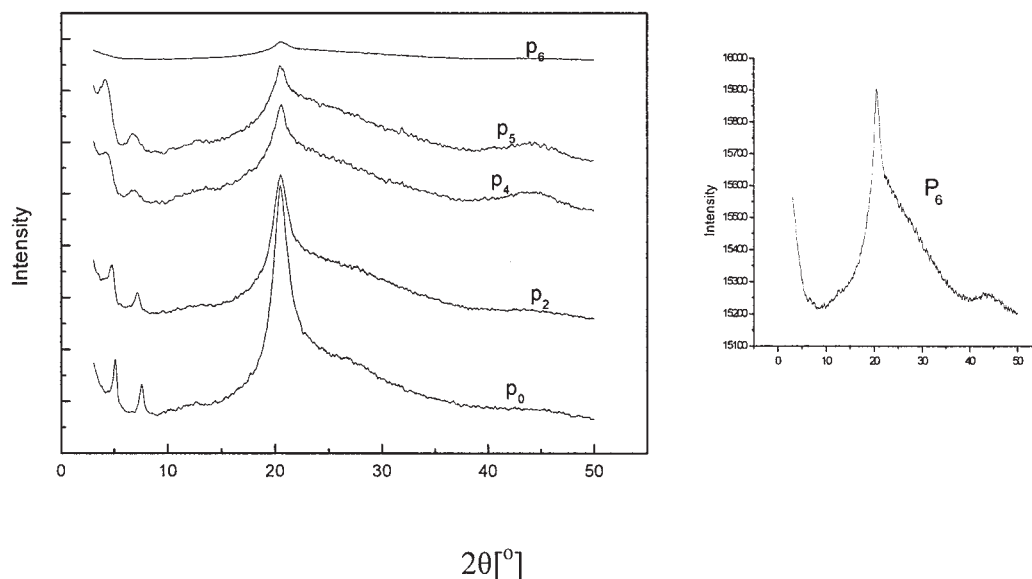


Figure 7 X-ray diffraction patterns of quenched samples.

indicate the second order reflection. The films of P_0 – P_5 showed another first sharp and then broad peak at 2θ of 20.59° ($d = 4.29 \text{ \AA}$), which are due first to high order (P_0 , P_1) and then to low order (P_2 – P_5) of the distance between the mesogenic side groups in the smectic layer.^{26,27} The peak of reflections for P_6 and P_7 are different. They have only sharp peaks at 20.59° ($d = 4.29 \text{ \AA}$). Combining polarizing microscopy with X-ray diffraction measurements may reveal²⁷ that polymer P_0 and elastomer P_1 were smectic B phase and elastomers P_2 – P_5 were smectic A phase, while P_6 and P_7 were cholesteric elastomers and P_8 displayed stress-induced birefringence. It may be concluded that the chirality of the chiral crosslinking agent has a strong effect on the phase of polymers during the increase of the contents of the crosslinker.

CONCLUSIONS

In this study, a series of new side-chain smectic and cholesteric LCEs containing smectic (S_B , S_A , S_C)–nematic monomer groups (M_1 , pentyloxy-4-undecanoyloxy-4'-benzoate) and chiral crosslinking agents (M_2 , isosorbide 4-allyloxybenzoyl bisate) were synthesized and characterized. All of the obtained polymers showed very wide mesophase temperature ranges and high thermal stability. The elastomers containing less than 15% of crosslinking units showed elasticity and reversible phase transition. The liquid crystalline phase of homopolymer and elastomers changed from S_B to S_A and then

cholesteric with increasing content of the chiral crosslinker. For P_0 – P_8 , the glass transition temperatures reduced first and then increased; the melting and isotropization temperatures and the ranges of the mesophase temperature decreased with increasing the content of crosslinking agent.

The authors are grateful to the National Natural Science Fundamental Committee of China and HI-Tech Research and development program (863) of China, the National Basic Research Priorities Program (973) of China, and the Science and Technology Research Major Project of Ministry of Education of China for financial support of this work.

References

1. Finkelmann, H.; Kock, H. J.; Rehage, G. *Makromol Chem Rapid Commun* 1981, 2, 317.
2. Zentel, R. *Angew Chem Adv Mater* 1989, 101, 1437.
3. Löffler, R.; Finkelman, H. *Macromol Chem Rapid Commun* 1990, 11, 321.
4. Davis, J. *J Mater Chem* 1993, 3, 551.
5. Zentel, R.; Reckert, G. *Makromol Chem* 1915 1986, 187.
6. Mitchell, R.; Davis, J. *Polymer* 1987, 28, 639.
7. Meier, W.; Finkelman H. *Condensed Matter News* 1992, 1, 15.
8. Meyer, R. B. *Mol Cryst Liq Cryst* 1997, 40, 33.
9. Lehmann, W.; Leister, N.; Hartmann, L.; Finkelmann, H. *Mol Cryst Liq Cryst* 1999, 328, 437.
10. Brehmer, M.; Zentel, R.; Wagenblast, G.; Siemensmeyer, K. *Macromol Chem Phys* 1994, 195, 1891.
11. Hiraoka, K.; Finkelmann, H. *Macromol Chem Phys* 1995, 196, 3197.
12. Broer, D.; J; Heynderickx, I. *Macromolecules* 1990, 23, 2474.
13. Zentel, R. *Polymer* 1992, 33, 4040.
14. Broer, D.; J; Lub, J.; Mol, G. *Nature* 1995, 378, 467.

15. Maxein, G.; Mayer, S.; Zentel, R. *Macromolecules* 1999, 32, 5747.
16. Hikmet, R. A. M.; Kemperman, H. *Nature* 1998, 392, 476.
17. Thomas, P.; Kurschner, K.; Strohhriegl, P. *Macromol Chem Phys* 1999, 200, 2480.
18. Peter, P. M. *Nature* 1998, 391, 745.
19. Hu, J. S.; Zhang, B. Y.; Sun, K.; Li, Q. Y. *Liq Cryst* 2003, 30, 1267.
20. Zhang, B. Y.; Hu, J. S.; Jia, Y. G.; Du, B. G. *Macromol Chem Phys* 2003, 204, 2123.
21. Hu, J. S.; Zhang, B. Y.; Jia, Y. G.; Chen, S. *Macromolecules* 2003, 36, 9060.
22. Kelly, S. M. *J Mater Chem* 1995, 5, 2047.
23. He, X. Z.; Zhang, B. Y.; Meng, F. B.; Lin, J. R. *J Appl Polym Sci* 2005, 96, 1204.
24. He, M. J.; Chen, X. W.; Dong, X. X. *High Polymer Physics*; Fudan University Press: Shang Hai, 1988; pp 68–75.
25. Teyssie, D.; Boileau, S. In *Silicon-Containing Polymers: The Science and Technology of Their Synthesis and Applications*; Jones, R.G.; Ando, W.; Chohnowski, J., Eds.; Kluwer Academic Publishers: Dordrecht, 2000; pp 593–561.
26. Stumpe, J.; Ziegler, A.; Berghahn, M.; Kricheldorf, H. R. *Macromolecules* 1995, 28, 5306.
27. Zhou, Q. F.; Wang, X. J. *Liquid Crystal Polymer*; Science Press: Beijing, 1999; pp 83–87, 104–108.